

See discussions, stats, and author profiles for this publication at: <https://www.researchgate.net/publication/264038784>

# Raman Spectroscopic Study of Antioxidant Pigments from Cup coral publicado

DATASET · JULY 2014

---

READS

46

8 AUTHORS, INCLUDING:



[Lenize Fernandes Maia](#)

Federal University of Juiz de Fora

29 PUBLICATIONS 305 CITATIONS

[SEE PROFILE](#)



[H. G. M. Edwards](#)

University of Bradford

752 PUBLICATIONS 11,673 CITATIONS

[SEE PROFILE](#)



[Luiz Fernando Cappa De Oliveira](#)

Federal University of Juiz de Fora

175 PUBLICATIONS 1,759 CITATIONS

[SEE PROFILE](#)

# Raman Spectroscopic Study of Antioxidant Pigments from Cup Corals *Tubastraea* spp.

Lenize F. Maia,<sup>†</sup> Gilson R. Ferreira,<sup>†,‡</sup> Regina C. C. Costa,<sup>†</sup> Nanci C. Lucas,<sup>§</sup> Rodolfo I. Teixeira,<sup>§</sup> Beatriz G. Fleury,<sup>||</sup> Howell G. M. Edwards,<sup>⊥</sup> and Luiz F. C. de Oliveira<sup>\*,†</sup>

<sup>†</sup>NEEM Núcleo de Espectroscopia e Estrutura Molecular, Departamento de Química, Instituto de Ciências Exatas, Universidade Federal de Juiz de Fora, 36036-330 Juiz de Fora, MG, Brazil

<sup>‡</sup>Faculdade de Ciências Médicas e da Saúde de Juiz de Fora, Hospital Maternidade Therezinha de Jesus - SUPREMA, 36033-003 Juiz de Fora, MG, Brazil

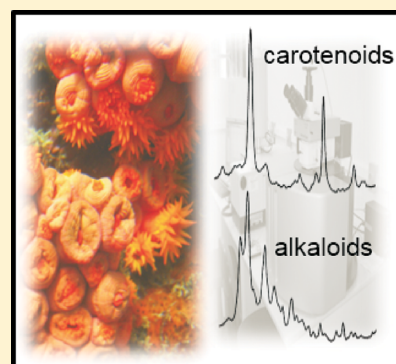
<sup>§</sup>Instituto de Química, Centro de Tecnologia, Universidade Federal do Rio de Janeiro, 21949-900 Rio de Janeiro, RJ, Brazil

<sup>||</sup>Departamento de Ecologia, IBRAG, Universidade do Estado do Rio de Janeiro, 20559-000 Rio de Janeiro, RJ, Brazil

<sup>⊥</sup>Centre for Astrobiology and Extremophile Research, School of Life Sciences, University of Bradford, Bradford BD7 1DP, United Kingdom

## S Supporting Information

**ABSTRACT:** Chemical investigation of nonindigenous *Tubastraea coccinea* and *T. tagusensis* by Raman spectroscopy resulted in the identification of carotenoids and indolic alkaloids. Comparison of Raman data obtained for the in situ and crude extracts has shown the potential of the technique for characterizing samples which are metabolic fingerprints, by means of band analysis. Raman bands at ca. 1520, 1160, and 1005 cm<sup>-1</sup> assigned to  $\nu_1(\text{C}=\text{C})$ ,  $\nu_2(\text{C}-\text{C})$ , and  $\rho_3(\text{C}-\text{CH}_3)$  modes were attributed to astaxanthin, and the band at 1665 cm<sup>-1</sup> could be assigned to the  $\nu(\text{C}-\text{N})$ ,  $\nu(\text{C}-\text{O})$ , and  $\nu(\text{C}-\text{C})$  coupled mode of the iminoimidazolinone from aplysinopsin. The antioxidant activity of the crude extracts has also been demonstrated, suggesting a possible role of these classes of compounds in the studied corals.



## INTRODUCTION

Scleractinians *Tubastraea coccinea* and *T. tagusensis* are ahermatypic corals nonindigenous to the South Atlantic<sup>1</sup> and are known to contain metabolites employed in a chemical defense role.<sup>2,3</sup> The introduced species have shown competitive advantages over native organisms, causing a negative impact in the receptor communities.<sup>2-5</sup> Species of genus *Tubastraea* are sources of fatty acids, sterols,<sup>5</sup> polyoxazole macrolides,<sup>6</sup> anthraquinone derivatives,<sup>7</sup> and alkaloids.<sup>5,7-10</sup> The orange *T. coccinea* and the yellow *T. tagusensis* collected on the Southwest Atlantic Coast (Angra dos Reis, RJ, Brazil) were investigated by Near Infrared Raman Spectroscopy (NIR-RS), which is a technique of choice for the identification of different types of molecules with a conjugated system of  $\pi$  electrons as reported for these corals. Raman spectra from in situ analysis showed several bands that could be attributed to two classes of compounds. Fingerprint bands from the Raman analysis indicated the presence of carotenoids and alkaloids containing an indolic group together with an iminoimidazolinone system characterized as aplysinopsins (Figure 1). This is the first report of the carotenoid astaxanthin (1) in tissues of the *Tubastraea* genus and the first characterization of indolic alkaloids by Raman spectroscopy. Aplysinopsin (2) and derivatives were

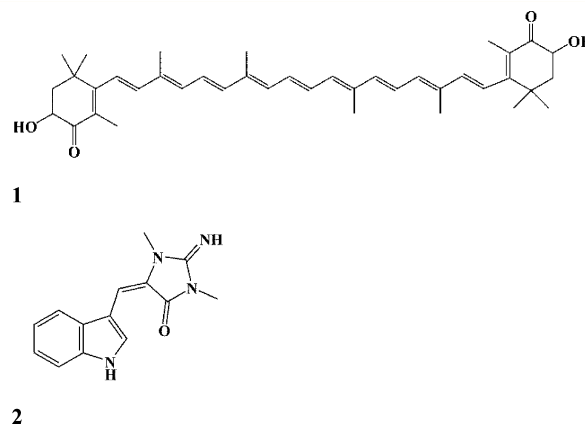


**Figure 1.** Metabolites identified from cup corals *T. coccinea* and *T. tagusensis* by Raman spectroscopy: (1) astaxanthin and (2) aplysinopsin.

Received: February 5, 2014

Revised: April 16, 2014

Published: April 17, 2014



**Table 1.** Main Observed Raman Bands with Laser Excitation at 1064 nm (cm<sup>-1</sup>) and Tentative Vibrational Assignments from Metabolites of Cup Corals *Tubastraea* spp., Pure Astaxanthin and Calculated Vibrational Wavenumbers of Aplysinopsin<sup>a</sup>

<i>T. coc.</i> in situ	<i>T. coc.</i> hexane	<i>T. coc.</i> MeOH	<i>T. tag.</i> in situ	<i>T. tag.</i> DCM	<i>T. tag.</i> MeOH	astax stand.	aplysins calcd	tentative assignments
1662w	1660w	1666s	1664m	1658m	1658m		1675	$\nu(\text{C}=\text{N})$ , $\nu(\text{C}=\text{O})$ , $\nu(\text{C}=\text{C})^b$
1619w	1596w	1620s	1618m	1623w	1621s		1632	$\nu(\text{C}=\text{O})$ , $\nu(\text{C}=\text{N})$ , $\nu(\text{C}-\text{N})$ , <sup>b</sup> $\nu(\text{C}=\text{C})^c$
1573w	1573w	1573w	1573w	1575w	1573w	1591w	1615	$\nu(\text{C}-\text{C})$ , $\delta_s(\text{CH})$ , $\delta_s(\text{NH})$ , <sup>c</sup> $\nu(\text{C}=\text{C})^d$
1519s	1521s	1510s	1519s	1521s	1521s	1512s	1546	$\nu(\text{C}-\text{C})$ , $\delta_s(\text{CH})$ , $\delta_s(\text{CH})_3$ , <sup>c</sup> $\nu(\text{C}=\text{C})^d$
1442w	1444m	1442w		1442m	1397w	1443w	1489	$\nu(\text{C}-\text{C})$ , $\delta_s(\text{CH})$ , $\delta_s(\text{CH})_3$ , <sup>b</sup> $\nu(\text{C}-\text{C})^d$
	1391w	1394w			1400w		1440	$\nu(\text{C}-\text{C})$ , $\delta_s(\text{NH})$ , $\delta_s(\text{CH})^c$
		1336m	1341w		1336m		1376	$\nu(\text{C}-\text{C})$ , $\delta_s(\text{CH})^c$
		1307w		1300w	1307w		1344	$\nu(\text{C}-\text{C})$ , $\delta_s(\text{CH})^c$
1274w	1276w		1276w	1276m	1274w	1276m	1301	$\delta_s(\text{CH}_3)$ , $\nu(\text{C}-\text{N})$ , <sup>b</sup> $\delta_s(\text{C}-\text{H})^d$
		1230w			1230w		1278	$\delta_s(\text{C}-\text{H})$ , $\nu(\text{C}-\text{N})$ , $\delta_s(\text{NH})^c$
1193m	1193m	1199w	1193w	1193m		1192m	1252	$\delta_{as}(\text{C}-\text{H})$ , $\nu(\text{C}-\text{N})$ , $\delta_s(\text{CH}_3)$ , <sup>b</sup> $\nu(\text{C}-\text{CH}_3)^d$
1085s			1085s					$\nu(\text{CO}_3^{2-})$
1158s	1157s	1158m	1157s	1157s	1158s	1156s	1171	$\nu(\text{N}-\text{CH}_3)$ , $\delta_s(\text{N}-\text{H})$ , $\nu(\text{C}-\text{N})$ , <sup>b</sup> $\nu(\text{C}-\text{C})^d$
			1052w		1048w		1102	$\delta_s(\text{CH})$
1006m	1006m	1014w	1006m	1008m	1008w	1006m	1043	$\nu(\text{C}-\text{N})$ , $\delta_s(\text{NH})$ , $\delta_s(\text{CH}_3)$ , <sup>b</sup> $\delta(\text{C}-\text{CH}_3)^d$
	958w		960w	961w	958w	967w	966	$\nu(\text{C}-\text{N})$ , $\delta_s(\text{NH})$ , $\delta_s(\text{N}-\text{CH}_3)$ , <sup>b</sup> $\delta(\text{C}-\text{H})^d$
705s			705w					$\nu(\text{CO}_3^{2-})$
					781w		778	$\omega_s(\text{CH})^c$
							733	ring breathing
		601w			603w		661	ring breathing

<sup>a</sup>Raman bands intensities: s, strong; m, medium; w, weak. <sup>b</sup>Iminodiazolinone. <sup>c</sup>Indole. <sup>d</sup>Carotenoid.<sup>45</sup>

previously reported for *T. coccinea* from Indo-Pacific reefs (Oahu, Hawaii)<sup>11</sup> which corroborated our findings (Figure 1). As commented above, Raman spectroscopy has been used successfully to characterize conjugated polyenes, as for instance carotenoids,<sup>12</sup> in different living systems such as plants,<sup>13–15</sup> algae,<sup>16</sup> lichens,<sup>17,18</sup> microorganisms,<sup>19</sup> corals,<sup>20</sup> crustaceans,<sup>21</sup> fishes,<sup>22</sup> and birds.<sup>23</sup> The carotenoid astaxanthin from *T. coccinea* hexane extract and indolic alkaloids from a methanol extract were unambiguously identified on the basis of theoretical calculations and experimental analysis performed in situ and with the crude extracts. Both compounds are known to possess antioxidant activity. One of the biological functions of astaxanthin in marine animals is the quenching of the oxygen singlet state and a scavenging of free radicals.<sup>24</sup> The antioxidant properties of the carotenoids have been largely studied in vitro due to the complexity of studying in vivo systems. The methods used to determine the antioxidant capacity of carotenoids generally adopt a homogeneous system and measure the capacity of the carotenoids to scavenge either peroxy radicals (ROO<sup>•</sup>)<sup>25–27</sup> or nonbiological radicals, such as ABTS<sup>27,28</sup> and to quench singlet oxygen (<sup>1</sup>O<sub>2</sub>).<sup>24,29–35</sup> Carotenoids have been recognized to be efficient singlet oxygen quenchers.

In this work we demonstrate by two different methods that the hexane extract containing astaxanthin and the methanol extract, which is rich in indole alkaloids, present in *T. coccinea* tissues are antioxidants. Measurement of the quenching rates of singlet oxygen using several carotenoids and hexane and methanol extracts in solution has been performed using a NIR <sup>1</sup>O<sub>2</sub> emission method. In addition, we have also evaluated the oxidation of the methanol extract by hydroxyl radicals in a Fenton-like reaction using V<sub>2</sub>O<sub>5</sub>/TiO<sub>2</sub>.

It is worth mentioning that Raman spectroscopy, using excitation near the electronic transition of the chemical system, is a suitable technique to characterize the presence of single and double carbon–carbon bonds in the delocalized  $\pi$  electronic system, where the C–C and C=C stretching vibrations are

the ones that appear enhanced in the Raman spectra, thus permitting the chemical characterization of very small amounts of compounds.<sup>36</sup> Our results demonstrate the power of the Raman spectroscopic technique for the identification of natural products containing carotenoids and alkaloids without the need to isolate the specific compounds, and the technique has been successfully applied for nondestructive in situ analysis of a wide range of samples<sup>13</sup> as well as for crude extracts and purified compounds.<sup>13,37–41</sup>

## EXPERIMENTAL SECTION

**Materials and Experimental Methods.** Raman spectroscopic measurements performed in situ and on the crude extracts from *Tubastraea* spp. were carried out using a Bruker RFS 100 instrument and a Nd<sup>3+</sup>/YAG laser operating at 1064 nm with a 4 cm<sup>-1</sup> spectral resolution, equipped with a Ge detector cooled with liquid nitrogen. In situ analysis of samples excited using 532 and 785 nm laser lines were recorded on a Horiba XploRA instrument equipped with an air-cooled charge-coupled detector (CCD) with the incident laser beam focused on the sample using a confocal microscope with a 50× objective. The laser output at the source was between 1 and 10 mW for the in situ measurements for the laser line at 532 nm and a higher laser power of 100 mW at the source was used for 785 nm excitation. The operating spectral resolution was 2 cm<sup>-1</sup> at both 532 and 785 nm wavelengths. In situ analysis of samples excited using 514 and 632.8 nm was performed on a Horiba Jobin Yvon LabRAM HR system, with a power of ca. 2 mW. HPLC analysis was performed on a Agilent Infinity 1200 Series HPLC that consisted of a quaternary pump 1260 VL, Model-G1312C, standard autosampler 1260ALS, Model-G1329B, with UV–vis detector 1260 VWD VL+, model-G1314C, and a Waters YMC carotenoid column (250 mm × 4.6 mm i.d. × 5  $\mu$ m) equipped with C<sub>30</sub> reversed phase material. The mobile phase setups consisted of three solvents (solvent A, acetonitrile; solvent B, methanol; solvent C,

chloroform). The detection of carotenoids (UV/vis detector) was accomplished at a wavelength of 430 nm. Data acquisition and processing were achieved with Agilent ChemiStation LC Systems software. The identification of the characteristic peaks was based on the relative retention times, namely, standard astaxanthin purchased from Sigma-Aldrich Co. (19.189 min), *T. coccinea* extracts ( $t_R$  = 19.742 min) and cochromatographed astaxanthin standard and *T. coccinea* extracts 19.282 min.

**Pure Astaxanthin (1).** UV (MeOH)  $\lambda_{\max}$  476 nm, UV (CHCl<sub>3</sub>)  $\lambda_{\max}$  491 nm. Raman bands see Table 1.

**Extract in Hexane from *T. coccinea*.** Orange gum; UV (MeOH)  $\lambda_{\max}$  402, 476 nm, UV (CHCl<sub>3</sub>)  $\lambda_{\max}$  387, 473 nm. Raman bands see Table 1.

**Extract in CH<sub>2</sub>Cl<sub>2</sub> from *T. coccinea*.** Dark orange gum; UV (MeOH)  $\lambda_{\max}$  384 nm. Raman bands see Table 1.

**Extract in MeOH from *T. coccinea*.** Yellow-brownish solid; UV (MeOH)  $\lambda_{\max}$  283, 385 nm. Raman bands see Table 1.

**Extract in CH<sub>2</sub>Cl<sub>2</sub> from *T. tagusensis*.** Yellow-brownish solid; UV (MeOH)  $\lambda_{\max}$  283, 393 nm. Raman bands see Table 1.

**Extract in MeOH from *T. tagusensis*.** Yellow-brownish solid; UV (MeOH)  $\lambda_{\max}$  283, 385 nm. Raman bands see Table 1.

**Calculations.** The structure of aplysinopsin was fully optimized in the gas phase at the B3LYP<sup>42,43</sup> level using a 6-311++G(d,p)<sup>44</sup> triple-quality basis set with inclusion of polarization functions for both the heavy and hydrogen atoms (hereafter abbreviated as B3LYP/6-311G(d,p). The geometry was considered as neutral species. The final geometry was characterized as minima on the potential energy surface through harmonic frequency calculations (all frequencies were found to be real). The Raman intensities were also calculated and the band spectra were simulated by fitting a Lorentzian type function<sup>45</sup> with parameters set to 10 cm<sup>-1</sup> for the average width of the peaks at half height and  $2 \times 10^{-6}$  mol cm<sup>-3</sup> for sample concentration. The spectra for all species were then assigned according to the normal-mode analysis. Frequency scaling was not needed once the predicted values and theoretical spectrum profiles were in satisfactory agreement with the experimentally observed spectra, allowing unambiguous band assignments. All calculations were carried out with Gaussian 09 program as installed in the computers of the Núcleo de Estudos em Química Computacional (NEQC-UFJF).<sup>46</sup>

**Catalytic Assays.** The hydrogen peroxide (Synth) decomposition study was carried out with 0.1 mL solution of H<sub>2</sub>O<sub>2</sub> (0.32 mol L<sup>-1</sup>) with 5 mg of catalyst V<sub>2</sub>O<sub>5</sub>/TiO<sub>2</sub> (6% of vanadium oxide) by measuring the formation of gaseous O<sub>2</sub> in a glass vial. The catalytic activity of the composite was evaluated by measuring the degradation rate of aqueous methylene blue (2.5 mL), monitored at a fixed wavelength of 633 nm in a UV/vis spectrophotometer, Shimadzu model UV1800. The oxidative reaction promotes a discoloration of the dye with time. Assays using methylene blue as a probe were performed in both the presence and absence of the MeOH extract (2.0 mg in 0.4 mL) in triplicate. The hexane extracts were not totally soluble in the reaction medium.

Time-resolved NIR emission of singlet molecular oxygen generated by photosensitizer. The third harmonic of a CryLas Nd:YAG HP 355-50 laser (pulse width of 1.0 ns and energy <150 mJ) was used as the excitation source for an aerated perinaphthenone (photosensitizer,  $A_{355}$  = 0.36) solution in CHCl<sub>3</sub>. In experiments using hexane extracts, samples were

solubilized in CHCl<sub>3</sub> and in experiments using methanol extracts samples were solubilized in EtOH.

The singlet oxygen emission at 1270 nm was measured with a spectrofluorometer (FS920 Edinburgh Instruments TMS300 monochromator). The detection system was equipped with a NIR Hamamatsu model H1033-45 photomultiplier. Slit 10 nm,  $T$  = 25.6 °C.

**Quenching of Singlet Oxygen.** Stock solutions of the quenchers were prepared so that it was only necessary to add microliter volumes to the sample cell to obtain appropriate concentrations of the quencher. The rate constants for the quenching of singlet oxygen emission with the different quenchers employed in this work were obtained from the Stern–Volmer plots after eq 1.

$$k_{\text{obs}} = k_0 + k_q[\text{Q}] \quad (1)$$

where  $k_0$  is the emission decay rate constant in the absence of quencher,  $k_{\text{obs}}$  is the emission decay rate constant in the presence of the quencher, and  $[\text{Q}]$  is the quencher concentration. Plots based on this equation were found to be linear, from which the value of  $k_q$  was determined. In a typical experiment, one adds microliter volumes of the quencher to a 3 mL solution of perinaphthenone (Table S3, Supporting Information).

**Collection.** Samples of *T. coccinea* and *T. tagusensis* (69.5 g) were collected at a depth of 1–4 m at Ilha dos Macacos, Angra dos Reis, RJ (S 23° 04.713'/W 42° 13.479'). After collection, the colonies were immediately frozen in dry ice and stored in a freezer.

**Extraction.** Frozen colonies of *T. coccinea* and *T. tagusensis* were freeze-dried prior to extraction. Soxhlet extraction of *T. coccinea* (78.8 g dry weight) with hexane followed by dichloromethane gave orange extracts (631.2 mg and 76.9 mg, respectively). Extraction with methanol furnished a brownish yellow extract (1.9 g). The Soxhlet extraction procedure with *T. tagusensis* (69.5 g dry weight) was carried out with dichloromethane and methanol giving extracts (76.9 mg and 1.91 g, respectively) with coloration patterns similar to those of *T. coccinea*.

## RESULTS AND DISCUSSION

**Spectroscopic Analysis.** Hexane crude extracts and in situ analysis of *Tubastraea* spp. specimens investigated by Raman spectroscopy using NIR laser excitation (1064 nm) showed vibrational bands characteristic of carotenoids<sup>13,14</sup> at ca. 1520, 1160, and 1005 cm<sup>-1</sup> assigned to  $\nu_1(\text{C}=\text{C})$ ,  $\nu_2(\text{C}-\text{C})$ , and  $\rho_3(\text{C}-\text{CH}_3)$  modes (Figures 2 and 3). The identification of the carotenoid content performed by HPLC (Figure 4) was based on the analysis of retention times of major peaks from hexane crude extract and standard astaxanthin (Sigma-Aldrich Co). Co-chromatography of pure astaxanthin and hexane crude extract confirmed the presence of astaxanthin in *T. coccinea* tissues. Comparison of Raman bands attributed to  $\nu_1(\text{C}=\text{C})$  of pure astaxanthin<sup>47</sup> with and samples from *Tubastraea* spp. showed a shift to higher wavenumbers from 1512 to ca. 1521 cm<sup>-1</sup>, respectively (Table 1). An explanation for this phenomena has already been proposed; the wavenumber position of the  $\nu_1$  band is dependent on the length of the polyconjugated chain and matrix effects as a consequence of chemical interactions in natural samples.<sup>14</sup>

Astaxanthin is a dominant carotenoid in marine animals<sup>48</sup> and is mostly found in fishes and crustaceans that have



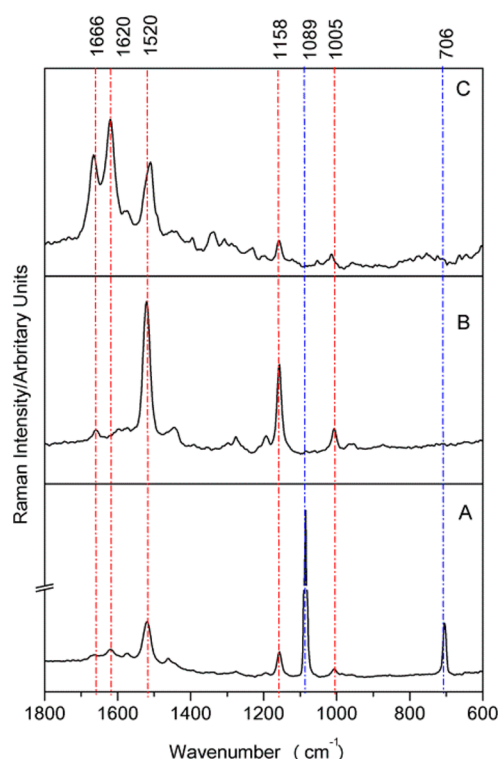


**Figure 2.** Raman spectra recorded at laser line 1064 nm of *T. coccinea*: A, in situ analysis; B, hexane extract; C, methanol extract.

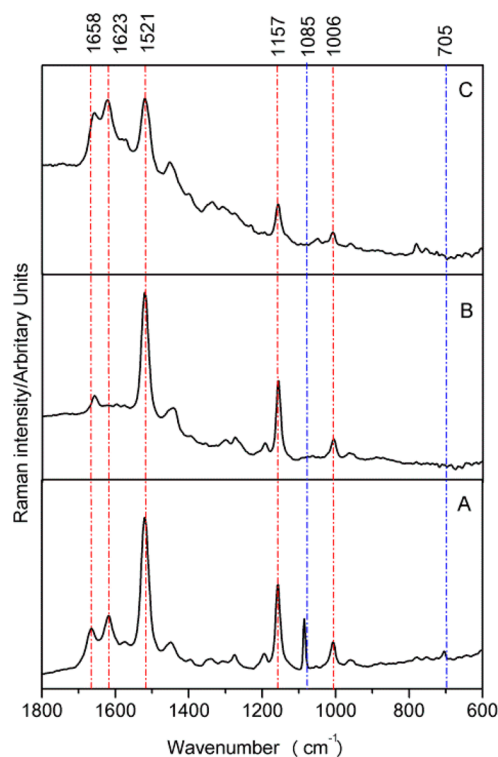


**Figure 3.** Raman spectra recorded at laser line 1064 nm of *T. tagusensis*: A, in situ analysis; B, hexane extract; C, methanol extract.

accumulated the carotenoid unchanged from either dietary or metabolic modifications.<sup>49–51</sup> The occurrence of astaxanthin in corals is restricted to a few species of zooxantharians,<sup>52</sup> to hydrocorals,<sup>53–55</sup> and to the octocorals *Simularia flexibilis*,<sup>56</sup> *Leptogorgia punicea*, and *Muricea atlantica*.<sup>41</sup> Perhaps the most

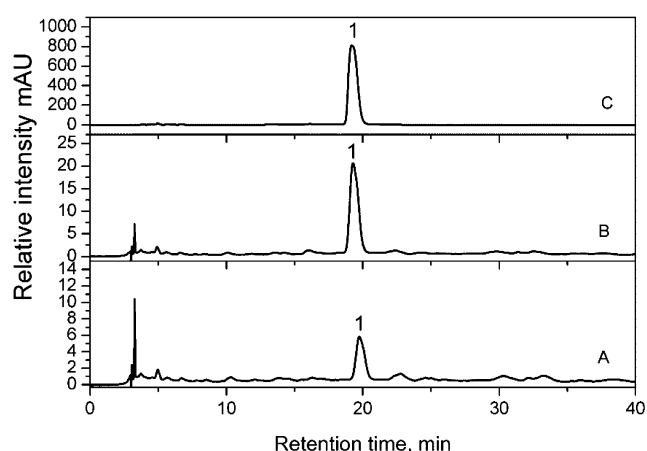


**Figure 4.** HPLC chromatograms of (a) *T. coccinea* hexane extract, (b) cochromatography of *T. coccinea* hexane extract with authentic astaxanthin, and (c) standard astaxanthin. The peak number refers to astaxanthin present in the analysis. Analytical conditions: waters YMC C<sub>30</sub> column (250 mm × 4.6 mm i.d. × 5 μm), flow rate 1 mL/min. Mobile phase: solvent A, acetonitrile; solvent B, methanol; solvent C, chloroform. UV/vis detector set at 430 nm.

relevant bioactive role of astaxanthin in animals is its ability to either quench or scavenge active oxygen species.<sup>24</sup> The function and origin of astaxanthin in *Tubastraea* spp. is unknown; pigmentation based on light-absorbing chromophores may act as a defense against oxygen singlet and free radical production. However, the in situ spectrum recorded here showed that astaxanthin occurs along with indole derivatives, which are also known to be effective antioxidants.<sup>57,58</sup> Raman spectroscopic analysis together with literature data have identified the presence of the indole alkaloids related to aplysinopsins previously described for *T. coccinea*<sup>11</sup> and sponge. These bioactive molecules are composed of an indole moiety and a creatinine based skeleton described as an iminoimidazolinone system. Methanol extracts of both species showed major bands at ca. 1665, 1620, 1574, 1510, 1452, 1441, 1396, 1338, 1158, and 1014 cm<sup>-1</sup>. Most of these bands were observed in the spectrum recorded in situ; however, bands at 1510, 1159, and 1014 cm<sup>-1</sup> were overlapped with carotenoid bands at ca. 1519, 1159, and 1005 cm<sup>-1</sup> (Figures 2 and 3). In situ spectra also showed bands at 1089 [ν(CO<sub>3</sub><sup>2-</sup>)] and 706 [ν(CO<sub>3</sub><sup>2-</sup>)] cm<sup>-1</sup> assigned to vibrational modes of carbonate ion in aragonite<sup>59</sup> (Figure 2 and 3). The tentative assignment of each band attributed to alkaloids has been proposed by comparison with the Raman bands in the literature<sup>60–62</sup> and theoretical calculations made for aplysinopsin [(2) Table 1, Figure 5]. Key bands from both moieties have been indicated in Table 1. The strong band at 1665 cm<sup>-1</sup> was attributed to [ν(C—N) + ν(C—O) + ν(C—C)] of the iminoimidazolinone. An intense band at 1619 cm<sup>-1</sup> was assigned to both the ν(C—C) of the indole nucleus and the [ν(C—O) + ν(C—N)] of the iminoimidazolinone system. The bands at 1510 cm<sup>-1</sup> due to [ν(C—N) + ν(C—C)] and at 1337 cm<sup>-1</sup> due to [ν(C—C) + δ<sub>s</sub>(C—H)] were assigned to the aromatic system of the indole. Bands at 1158 and 1014 cm<sup>-1</sup> were assigned to [ν(N—CH<sub>3</sub>) + δ<sub>s</sub>(N—H) + ν(C—N) + ν(C—C)], and [ν(C—N) + δ<sub>s</sub>(NH) + δ<sub>s</sub>(CH<sub>3</sub>)], respectively, of the iminoimidazolinone. Figure 6 shows a correlation between the experimental and the predicted frequencies from theoretical calculations made on aplysinopsin. The experimental Raman shifts appear to have shifted linearly

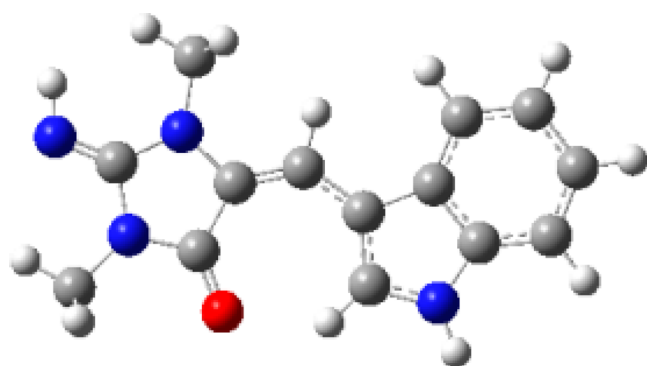


**Figure 5.** Optimized structure for aplysinopsin at theoretical level B3LYP/6-311++G(d,p).

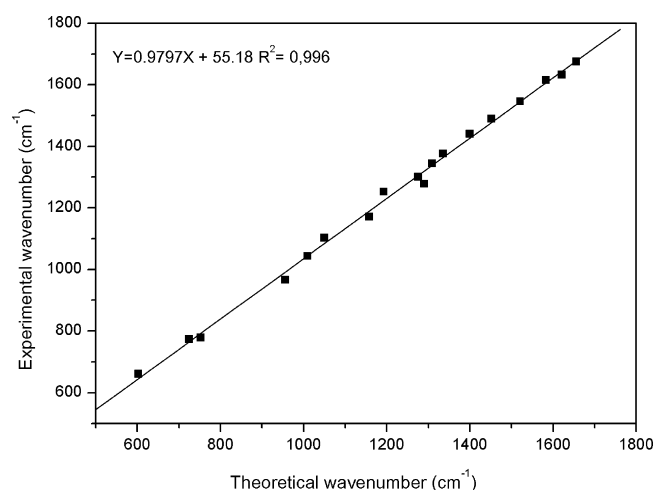


**Figure 6.** Correlation coefficient and scatter plot of Raman frequencies between experimental data from *T. coccinea* methanol extract and theoretical data from aplysinopsin.

and are in good agreement ( $R^2 = 0.996$ ) with the theoretical data. Both pigments were identified by NIR-RS (1064 nm) in tissues of the orange *T. coccinea* and the yellow *T. tagusensis*. However, Raman measurements of *T. coccinea* tissues made with different laser lines at 514, 532, 632.8, 785, and 1064 nm showed fingerprint bands attributed to carotenoids and carbonate ion (Figure 7). It is important to note that under resonance conditions, such as the Raman spectra obtained with green light excitations, some of the vibrational modes that are involved with the electronic transition are the ones that appear with their intensity enhanced, according to the theory predict by inelastic light scattering;<sup>63–66</sup> in this case, the literature has demonstrated that the chromophoric species are the C—C, C=C, and C—CH<sub>3</sub> chemical groups present in the structure of carotenoids.<sup>67</sup>

Aplysinopsins are yellow pigments isolated from sponges,<sup>69</sup> mollusc,<sup>10</sup> and scleractinians<sup>70–72</sup> whereas astaxanthins are reddish orange pigments widely distributed in nature.<sup>48</sup> It is possible that either aplysinopsin or astaxanthin from *T. coccinea* and *T. tagusensis* could be involved in the coloration of their tissues and even the coloration of their predators as the nudibranch *Phestilla melanobranchia*, which feeds on *T. coccinea*, exhibit the same color pattern<sup>11</sup> as well as the same chemical composition.<sup>71</sup> Aplysinopsins are biologically active against cancer cells, are antiplasmodial and antimicrobial, and act as modulators in neurotransmission.<sup>10</sup> Chemical and ecological

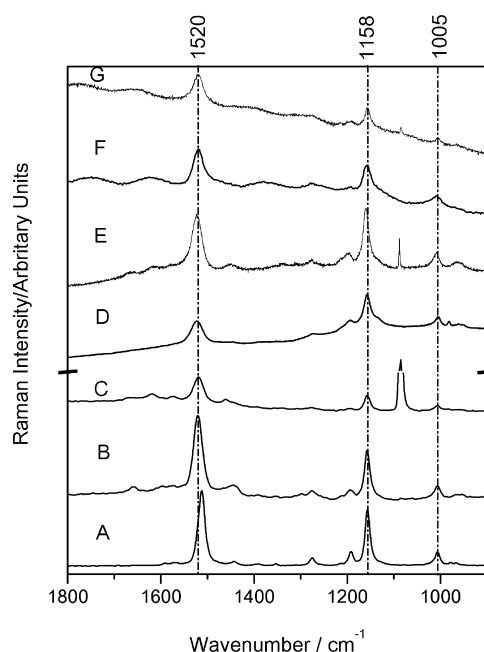


**Figure 7.** Raman spectra recorded at different laser lines: (A) standard astaxanthin recorded at 1064 nm. *T. coccinea* analysis: (B) hexane extract at 1064 nm; (C) in situ at 1064 nm; (D) in situ at 785 nm; (E) in situ at 632.8 nm; (F) in situ at 532 nm; (G) in situ at 514 nm.

experimental data have demonstrated that methanol crude extracts from *T. coccinea* and *T. tagusensis*, which are rich in alkaloids were effective against fish fouling and induced different responses in the fouling community, inhibiting or enhancing settlement, survival or the growth of different taxa.<sup>2</sup> Alcoholic extracts and aplysinopsin derivatives from *T. faulkneri* were toxic to larvae of potential competitors and antimicrobial against marine bacteria and cyanobacteria.<sup>72</sup> The antioxidant activity of 6-bromo-2'-de-N-methylaplysinopsin isolated from the sponge *Hyrtios* sp. has been reported previously.<sup>58</sup>

In this work, we have evaluated the antioxidant activity of crude extracts from *T. coccinea* against hydroxyl radical species and singlet molecular oxygen. Hydroxyl radicals were generated from hydrogen peroxide by a catalysis system using vanadium pentoxide (V<sub>2</sub>O<sub>5</sub>) supported on titanium dioxide (TiO<sub>2</sub>). V<sub>2</sub>O<sub>5</sub> is an important metal oxide catalyst and in combination with TiO<sub>2</sub> is useful for photocatalytic reactions.<sup>73</sup> The composite layers are biologically and chemically inert, in addition vanadium peroxide complexes are known to be strong oxidants capable of decomposing hydrogen peroxide even in biological systems.<sup>74</sup> The hydrogen peroxide decomposition was investigated in the presence of the catalyst with the addition of the crude extracts and using methylene blue as a probe. The oxidation of methylene blue in the presence of hydroxyl radicals was monitored by absorption at 663 nm and the discoloration plots showed a color reduction of 42.83% over the time of the experiment (Figure 8). However, a lower activity for methylene blue oxidation was observed in the presence of hydroxyl radicals and of the MeOH crude extract. Figure 8 shows a color retention of 70.61% against 42.83% in the absence of the crude extract at the end of 1 h. The inhibition of discoloration by the MeOH extract suggested that radical species reacted more efficiently with the mixture of alkaloids than with the methylene blue.

To evaluate the antioxidant activity of different reactive oxygen species, the ability of crude extracts in quenching singlet

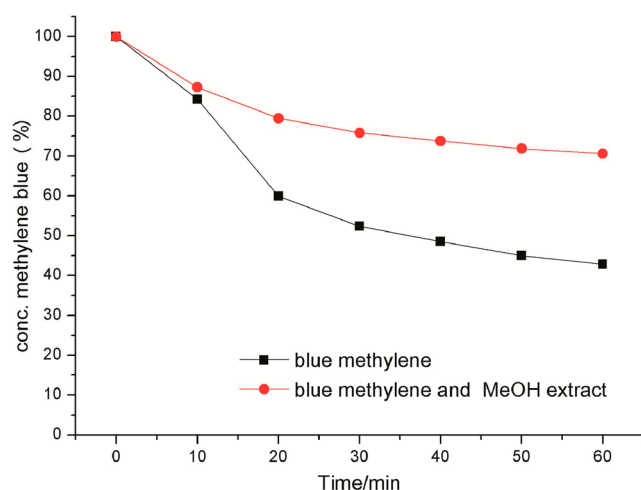


**Figure 8.** Discoloration plot of methylene blue oxidation in the presence of  $\text{H}_2\text{O}_2$  and catalyst in the absence and presence of *T. coccinea* methanol crude extracts.

oxygen was tested. Singlet oxygen can be formed through an energy transfer process from a suitable donor, usually a sensitizer in the triplet excited state ( $^3\text{Sens}^*$ ). A tiny fraction of  $^1\text{O}_2$  molecules undergoes radioactive decay, thereby emitting a photon in the near-infrared (NIR). This extremely weak phosphorescence, centered at 1270 nm, provides the means for the most direct and unambiguous method for  $^1\text{O}_2$  detection. In this study singlet oxygen was generated using perinaphthenone as photosensitizer. After laser excitation (355 nm), the aerated chloroform solution of perinaphthenone emits phosphorescence at 1270 nm that decays with a rate constant ( $k_0$ ) of approximately  $12\,000\text{ s}^{-1}$ , corresponding to a lifetime of around  $85\text{ }\mu\text{s}$ . The lifetime of state shows a strong solvent dependence. The experimental values observed here ranging from  $83.80$  to  $88.97\text{ }\mu\text{s}$  (Table S1–4, Supporting Information) is lower than the lifetime of singlet oxygen in chloroform (literature value is  $\tau_\Delta = 207\text{ }\mu\text{s}$ ).<sup>75</sup> Decreasing in lifetime of singlet oxygen in solution has already been reported and may be attributed, among other reasons, to subtle variations in experimental condition.<sup>55</sup>

**Quenching of Singlet Oxygen.** In homogeneous media, the singlet oxygen reaction with carotenoids can involve physical and/or chemical processes. In this study, the total (physical and chemical) quenching rate constant,  $k_q$ , for the reaction of  $^1\text{O}_2$  was performed with different quenchers, such as  $\beta$ -carotene, astaxanthin, hexane extract in , and MeOH extract in EtOH as solvent. Quenching rates were obtained from the experimentally measured first-order decay of  $^1\text{O}_2$  phosphorescence at 1270 nm in the absence and the presence of the quencher. The singlet oxygen decays obtained in chloroform with perinaphthenone in the absence and in the presence of the hexane extract is shown in Figure 9, and those of  $\beta$ -carotene and astaxanthin in Figures S1 and S2 (Tables S1 and S2) of the Supporting Information, respectively. All decays fit first-order kinetics from which singlet oxygen lifetimes were computed. The  $k_q$  values were calculated from the slope of the Stern–Volmer plots according to eq 1 (Figure 9 and Figures S1 and S2 of the Supporting Information). Quenching of the singlet oxygen by the hexane extract occurred with a rate constant approaching that of diffusion control ( $k_{\text{diff}}(\text{CHCl}_3) = 1.12 \times 10^{10}\text{ L mol}^{-1}\text{ s}^{-1}$ ),<sup>75</sup> which is in accord with the physical nature of the energy transfer process. The results obtained with the

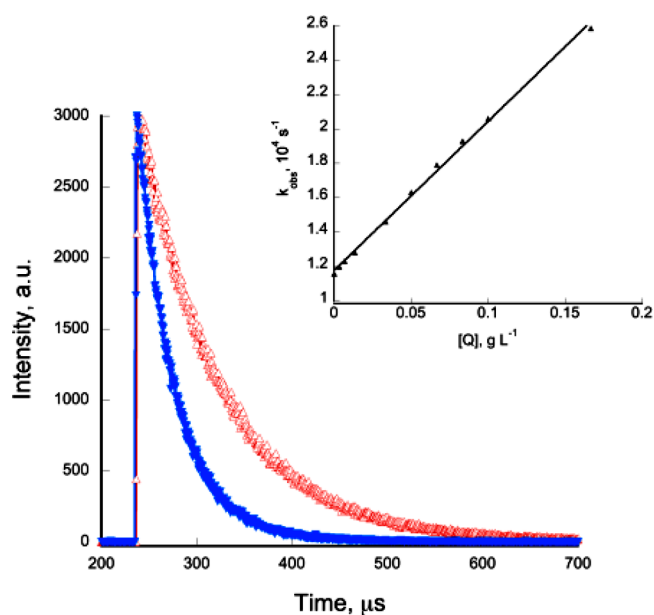


**Figure 9.** Singlet oxygen decays in the absence ( $\Delta$ ) and in the presence of  $1.17\text{ g L}^{-1}$  ( $\nabla$ ) of hexane extract, perinaphthenone as sensitizer, and chloroform as solvent. Inset: Stern–Volmer plot according to eq 1.

MeOH extract did not quench singlet oxygen showing rate constant and lifetime similar to that of the observed for the probe (Figure S3, Table S3, Supporting Information). For comparison, Table 2 shows the literature values of  $k_q$  for the carotenoids in  $\text{CHCl}_3$ .<sup>24</sup>

**Table 2.** Rate Constants of Quenching of Singlet Oxygen by the Investigated Carotenoids

quencher	$k_q$ (obs)	$k_q$ , $\text{L mol}^{-1}\text{ s}^{-1}$
$\beta$ -carotene <sup>72</sup>	$(1.63 \pm 0.10) \times 10^{10}\text{ L mol}^{-1}\text{ s}^{-1}$	$1.1 \times 10^{10}$
astaxanthin <sup>72</sup>	$(2.18 \pm 0.09) \times 10^{10}\text{ L mol}^{-1}\text{ s}^{-1}$	$1.2 \times 10^{10}$
hexane extract	$(8.68 \pm 0.15) \times 10^4\text{ L g}^{-1}\text{ s}^{-1}$	

The systems used to assay the antioxidant activity of pigments from the cup corals showed selectivity of the reactive oxygen species tested toward the chemical nature of compounds. Scavenging of hydroxyl radical was demonstrated in experiments performed with methanol extract rich in alkaloids and quenching of singlet oxygen was observed only in assays with hexane extracts containing carotenoids.

## CONCLUSIONS

The investigation by Raman spectroscopy of the pigment composition of orange tissues from *T. coccinea* and yellow tissues of *T. tagusensis* revealed that they are due to carotenoids and indolic alkaloids such as aplysinopsin derivatives. Occurrence of aplysinopsin derivative in *T. coccinea* tissues is known; however, this is the first report to *T. tagusensis*. Also new is the presence of astaxanthin in tissues of the genus *Tubastraea*, although it is a common compound in marine organisms, the identification have been neglected. In our work we used Raman spectroscopy, which is the technique of choice in studying polyconjugated system as identified in cup corals. Aplysinopsin carbon skeleton showed fingerprint bands in Raman spectra that could be used as a chemical marker, because this class of bioactive alkaloid may occur in other

marine organisms rather than sponges, corals, and their predators. The data we presented here has also shown that pigments in *T. coccinea* and *T. tagusensis* are used for ornamental purposes and may be implied in physiological processes. The antioxidant assays provided a clue that *Tubastraea* spp. use compounds from different chemical classes for different oxidative systems. Methanol extract rich in alkaloids were effective in scavenging hydroxyl radical, whereas hexane extracts containing carotenoids were effective in quenching of singlet oxygen.

## ■ ASSOCIATED CONTENT

### ■ Supporting Information

Experimental conditions and measured parameters of quenching oxygen singlet by  $\beta$ -carotene, astaxanthin, hexane extract, and methanol extract (Tables S1–S5), singlet oxygen decays (Figures S1–S5), and complete ref 46 are available free of charge via the Internet at <http://pubs.acs.org>.

## ■ AUTHOR INFORMATION

### Corresponding Author

\*L. F. C. de Oliveira: e-mail, [luiz.oliveira@ufjf.edu.br](mailto:luiz.oliveira@ufjf.edu.br); tel, +55 (32) 3229-3310; fax, +55 (32) 3229-3310.

### Notes

The authors declare no competing financial interest.

## ■ ACKNOWLEDGMENTS

The authors thank CNPq, CAPES/Ciências do Mar 1137/2010 and FAPEMIG (Brazilian agencies) for financial support. The authors also thank Ari Miranda da Silva (Núcleo de Pesquisa de Produtos Naturais-NPPN, UFRJ) for the HPLC analysis and Horiba do Brasil for the loan of the Raman spectrometer with visible excitation.

## ■ REFERENCES

- (1) De Paula, A. F.; Creed, J. C. Two Species of the Coral *Tubastraea* (Cnidaria, Scleractinia) in Brazil: A Case of Accidental Introduction. *Bull. Mar. Sci.* **2004**, *74*, 175–183.
- (2) Lages, B. G.; Fleury, B. G.; Pinto, A. C.; Creed, J. C. Chemical Defenses Against Generalist Fish Predators and Fouling Organisms in Two Invasive Ahermatypic Corals in the Genus *Tubastraea*. *Mar. Ecol.* **2010**, *31*, 473–482.
- (3) Lages, B. G.; Fleury, B. G.; Rezende, C. M.; Pinto, A. C.; Creed, J. C. Chemical Composition and Release in Situ Due to Injury of the Invasive Coral *Tubastraea* (Cnidaria, Scleractinia). *Brazilian Journal of Oceanography* **2010**, *58*, 47–56.
- (4) Lages, B. G.; Fleury, B. F.; Menegola, C.; Creed, C. J. Change in Tropical Rocky Shore Communities Due to an Alien Coral Invasion. *Mar. Ecol.: Prog. Ser.* **2011**, *438*, 85–96.
- (5) Lages, B.; Fleury, B. G.; Hovell, A. C.; Rezende, C. M.; Pinto, A. C.; Creed, J. C. Proximity to Competitors Changes Secondary Metabolites of Non-indigenous Cup Corals, *Tubastraea* spp., in the Southwest Atlantic. *Mar. Biol. (Heidelberg, Ger.)* **2012**, *159*, 1551–1559.
- (6) Rashid, M. A.; Gustafson, K. R.; Cardeilina, J. H.; Boyd, M. R. Mycalolides D and E, New Cytotoxic Macrolides from a Collection of the Stony Coral *Tubastrea faulkneri*. *J. Nat. Prod.* **1995**, *58*, 1120–1125.
- (7) Radhika, S.; Alam, M.; Wellington, G. M. Secondary Metabolites of the Non-Symbiotic Coral *Tubastrea micrantha*. *J. Chem. Res. (S)* **1986**, *12*, 450–451.
- (8) Sakai, R.; Higa, T. Tubastrine, a New Guanidinostyrene From the Coral *Tubastrea aurea*. *Chem. Lett.* **1987**, *16*, 127–128.
- (9) Iwagawa, T.; Miyazaki, M.; Okamura, H.; Nakatani, M.; Doe, M.; Takemura, K. Three Novel Bis(indole) Alkaloids From a Stony Coral, *Tubastraea* sp. *Tetrahedron Lett.* **2003**, *44*, 2533–2535.
- (10) Bialonska, D.; Zjawiony, J. Aplysinopsins - Marine Indole Alkaloids: Chemistry, Bioactivity and Ecological Significance. *Mar. Drugs* **2009**, *7*, 166–183.
- (11) Okuda, R. K.; Klein, D.; Kinnel, R. B.; Li, M.; Scheuer, P. J. Marine Natural Products: the Past Twenty Years and Beyond. *Pure Appl. Chem.* **1982**, *54*, 1907–1914.
- (12) Ermakov, I. V.; Sharifzadeh, M.; Bernstein, P. S.; Gerllermann, W. Application of Resonance Raman Spectroscopy to the Detection of Carotenoids In Vivo. In *Carotenoids Physical, Chemical, and Biological Functions and Properties*; Landrum, J. T., Eds.; CRC Press: Boca Raton, FL, USA, 2009.
- (13) Schulz, H.; Baranska, M. Identification and Quantification of Valuable Plant Substances by IR and Raman Spectroscopy. *Vibr. Spectrosc.* **2007**, *43*, 13–25.
- (14) De Oliveira, V. E.; Castro, H. V.; Edwards, H. G. M.; De Oliveira, L. F. C. Carotenes and Carotenoids in Natural Biological Samples: A Raman Spectroscopic Analysis. *J. Raman Spectrosc.* **2010**, *41*, 642–650.
- (15) Britton, G.; Liaaen-Jensen, S.; Pfander, H. *Carotenoids*; Birkhauser Verlag: Basel, Switzerland, 1995.
- (16) Parab, N. D. T.; Tomar, V. Raman Spectroscopy of Algae: A review. *J. Nanomed. Nanotechnol.* **2012**, *3*, 1–7.
- (17) Edwards, H. G. M.; Moody, C. D.; Jorge Villar, S. E.; Wynn-Williams, D. D. Raman Spectroscopic Detection of Key Biomarkers of Cyanobacteria and Lichen Symbiosis in Extreme Antarctic Habitats: Evaluation for Mars Lander Missions. *Icarus* **2005**, *174*, 560–571.
- (18) De Oliveira, L. F. C.; Pinto, P. C. C.; Marcelli, M. P.; Dos Santos, H. F.; Edwards, H. G. M. The Analytical Characterization of a Depside in a Living Species: Spectroscopic and Theoretical Analysis of Lecanoric Acid Extracted From *Parmotrema tinctorum* Del. ex Nyl. Lichen. *J. Mol. Struct.* **2009**, *920*, 128–133.
- (19) Rösch, P.; Harz, M.; Schmitt, M.; Peschke, K.-D.; Ronneberger, O.; Burkhardt, H.; Motzkus, H. W.; Lankers, M.; Hofer, S.; Thiele, H.; Popp, J. Chemotaxonomic Identification of Single Bacteria by Micro-Raman Spectroscopy: Application to Clean-Room-Relevant Biological Contaminations. *Appl. Environ. Microbiol.* **2005**, *71*, 1626–1637.
- (20) Karampelas, S.; Fritsch, E.; Rondeau, B.; Andouche, A.; Métié, B. Identification of the Endangered Pink-to-red *Cladophora* Corals by Raman Spectroscopy. *Gems Gemol.* **2009**, *45*, 48–52.
- (21) Britton, G.; Weesie, R. J.; Askin, D.; Warburton, J. D.; GallardoGuerrero, L.; Jansen, F. J.; deGroot, H. J. M.; Lugtenburg, J.; Cornard, J. P.; Merlin, J. C. Carotenoid Blues: Structural Studies on Carotenoproteins. *Pure Appl. Chem.* **1997**, *69*, 2075–2084.
- (22) Wold, J. P.; Marquardt, B. J.; Dable, B. K.; Robb, D.; Hatlen, B. Rapid Quantification of Carotenoids and Fat in Atlantic Salmon (*Salmo salar* L.) by Raman Spectroscopy and Chemometrics. *Appl. Spectrosc.* **2004**, *58*, 395–403.
- (23) Veronelli, M.; Zerbi, G.; Stradi, R. In situ Resonance Raman Spectra of Carotenoids in Bird's Feathers. *J. Raman Spectrosc.* **1995**, *26*, 683–692.
- (24) Miki, W. Biological Functions and Activity of Animal Carotenoids. *Pure Appl. Chem.* **1991**, *63*, 141–146.
- (25) Naguib, Y. M. A. Antioxidant Activities of Astaxanthin and Related Carotenoids. *J. Agric. Food Chem.* **2000**, *48*, 1150–1154.
- (26) Rodrigues, E.; Mariutti, L. R. B.; Chiste, R. C.; Mercadante, A. Z. Development of a Novel Micro-assay for Evaluation of Peroxyl Radical Scavenger Capacity: Application to Carotenoids and Structure-Activity Relationship. *Food Chem.* **2012**, *135*, 2103–2111.
- (27) Mueller, L.; Froehlich, K.; Boehm, V. Comparative Antioxidant Activities of Carotenoids Measured by Ferric Reducing Antioxidant Power (FRAP), ABTS Bleaching Assay (Alpha TEAC), DPPH Assay and Peroxyl Radical Scavenging Assay. *Food Chem.* **2011**, *129*, 139–148.



- (28) Miller, N. J.; Sampson, J.; Candeias, L. P.; Bramley, P. M.; Rice, E. C. A. Antioxidant Activities of Carotenes and Xanthophylls. *FEBS Letters* **1996**, *384*, 240–242.
- (29) Foote, C. S.; Denny, R. W. Chemistry of singlet oxygen 7 quenching by beta-carotene. *J. Am. Chem. Soc.* **1968**, *90*, 6233–6235.
- (30) Di Mascio, P.; Kaiser, S.; Sies, H. Lycopene as the Most Efficient Biological Carotenoid Singlet Oxygen Quencher. *Arch. Biochem. Biophys.* **1989**, *274*, 532–538.
- (31) Edge, R.; McGarvey, D. J.; Truscott, T. G. The Carotenoids as Anti-oxidants - a Review. *J. Photochem. Photobiol., B* **1997**, *41*, 189–200.
- (32) Di Mascio, P.; Sundquist, A. R.; Devasagayam, T. P. A.; Sies, H. Assay of Lycopene and Other Carotenoid as Singlet Oxygen Quenchers. *Methods Enzymol.* **1992**, *213*, 429–438.
- (33) Pinto, E.; Catalani, L. H.; Lopes, N. P.; Di Mascio, P.; Colepicolo, P. Peridinin as the Major Biological Carotenoid Quencher of Singlet Oxygen in Marine Algae *Gonyaulax Polyedra*. *Biochem. Biophys. Res. Commun.* **2000**, *268*, 496–500.
- (34) Ouchi, A.; Aizawa, K.; Iwasaki, Y.; Inakuma, T.; Terao, J.; Nagaoka, S.-i.; Mukai, K. Kinetic Study of the Quenching Reaction of Singlet Oxygen by Carotenoids and Food Extracts in Solution. Development of a Singlet Oxygen Absorption Capacity (SOAC) Assay Method. *J. Agric. Food Chem.* **2010**, *58*, 9967–9978.
- (35) Rodrigues, E.; Mariutti, L. R. B.; Mercadante, A. Z. Scavenging Capacity of Marine Carotenoids Against Reactive Oxygen and Nitrogen Species in a Membrane-Mimicking System. *Mar. Drugs* **2012**, *10*, 1784–1798.
- (36) Vitek, P.; Jehlička, J.; Edwards, H. M.; Osterrothová, K. Identification of  $\beta$ -carotene in an Evaporitic Matrix—Evaluation of Raman Spectroscopic Analysis for Astrobiological Research on Mars. *Anal. Bioanal. Chem.* **2009**, *393*, 1967–1975.
- (37) De Oliveira, L. F. C.; Edwards, H. G. M.; Vellozo, E. S.; Nesbitt, M. Vibrational Spectroscopic Study of Brazilin and Brazilin, the Main Constituents of Brazilwood From Brazil. *Vibr. Spectrosc.* **2002**, *28*, 243–249.
- (38) Schrader, B.; Schulz, H.; Baranska, M.; Andreev, G. N.; Lehner, C.; Sawatzki, J. Non-destructive Raman Analyses – Polyacetylenes in Plants. *Spectrochim. Acta Part A* **2005**, *61*, 1395–1401.
- (39) Maia, L. F.; Fleury, B. G.; Lages, B. G.; Barbosa, J. P.; Pinto, Â. C.; Castro, H. V.; De Oliveira, V. E.; Edwards, H. G. M.; De Oliveira, L. F. C. Identification of Reddish Pigments in Octocorals by Raman Spectroscopy. *J. Raman Spectrosc.* **2011**, *42*, 653–658.
- (40) Maia, L. F.; De Oliveira, V. E.; De Oliveira, M. E. R.; Fleury, B. G.; De Oliveira, L. F. C. Polyenic Pigments From the Brazilian Octocoral *Phyllogorgia Dilatata* Esper, 1806 Characterized by Raman Spectroscopy. *J. Raman Spectrosc.* **2012**, *43*, 161–164.
- (41) Maia, L. F.; De Oliveira, V. E.; Oliveira, M. E. R.; Reis, F. D.; Fleury, B. G.; Edwards, H. G. M.; De Oliveira, L. F. C. Colour Diversification in Octocorals Based on Conjugated Polyenes: A Raman Spectroscopic View. *J. Raman Spectrosc.* **2013**, *44*, 560–566.
- (42) Becke, A. D. Density-functional Exchange-energy Approximation With Correct Asymptotic Behavior. *Phys. Rev. A* **1988**, *38*, 3098–3100.
- (43) Lee, C.; Yang, W.; Parr, R. G. Development of the Colle-Salvetti Correlation-Energy Formula Into a Functional of the Electron Density. *Phys. Rev. B* **1988**, *37*, 785–789.
- (44) Gordon, M. S.; Binkley, J. S.; Pople, J. A.; Pietro, W. J.; Hehre, W. J. Self-Consistent Molecular-orbital Methods. 22. Small Split-valence Basis Sets for Second-row Elements. *J. Am. Chem. Soc.* **1982**, *104*, 2797–2803.
- (45) Dos Santos, H. F.; De Almeida, W. B.; Do Val, A. M. G.; Guimarães, A. C. Espectro Infravermelho e Análise Conformacional do Composto 3-Fenil-2-oxo-1,2,3-oxatiazolidina. *Quím. Nova* **1999**, *22*, 732–736.
- (46) Frisch, M. J.; Trucks, G. W.; Schlegel, H. B.; Scuseria, G. E. *Gaussian 09*, Revision A.02; Wallingford, CT, USA, 2009.
- (47) Weesie, R. J.; Merlin, J. C.; Lugtenburg, J.; Britton, G.; Jansen, F. J. H. M.; Cornard, J. P. Semiempirical and Raman Spectroscopic Studies of Carotenoids. *Biospectroscopy* **1999**, *5*, 19–33.
- (48) Matsuno, T. Aquatic Animal Carotenoids. *Fisheries Sci.* **2001**, *67*, 771–783.
- (49) Goodwin, T. W. Metabolism, Nutrition, and Function of Carotenoids. *Annu. Rev. Nutr.* **1986**, *6*, 273–297.
- (50) Van Nieuwerburgh, L.; Wänstrand, I.; Liu, J.; Snoeijs, P. Astaxanthin Production in Marine Pelagic Copepods Grazing on Two Different Phytoplankton Diets. *J. Sea Res.* **2005**, *53*, 147–160.
- (51) Sommer, F.; Agurto, C.; Henriksen, P.; Kjørboe, T. Astaxanthin in the Calanoid Copepod *Calanus helgolandicus*: Dynamics of Esterification and Vertical Distribution in the German Bight, North Sea. *Mar. Ecol.: Prog. Ser.* **2006**, *319*, 167–173.
- (52) Czczuga, B. Presence of  $\beta$ -carotene and a Number of Xanthophylls in *Hyale Perieri* (Crustacea: Amphipoda) from the Black Sea. *Mar. Biol.* **1970**, *6*, 117–120.
- (53) Fox, D. L. Relative chemical stability of inorganically conjugated astaxanthin. *Comp. Biochem. Physiol. Part B* **1976**, *55*, 137–139.
- (54) Zagalsky, P. F.; Herring, P. J. Studies on Bleu Astaxanthin-protein of *Velella-velella* (Coelenterata-Chondrophora). *Philos. Trans. R. Soc. B* **1977**, *279*, 289–326.
- (55) Rønneberg, H.; Fox, D. L.; Liaen-Jensen, S. Animal Carotenoids—Carotenoproteins From Hydrocorals. *Comp. Biochem. Physiol. Part B* **1979**, *64*, 407–408.
- (56) Khalesi, M. K.; Lamers, P. P. Partial Quantification of Pigments Extracted From the Zooxanthellate Octocoral *Sinularia Flexibilis* at Varying Irradiances. *Biology* **2010**, *65*, 681–687.
- (57) Herraiz, T.; Galisteo, J. Endogenous and Dietary Indoles: A Class of Antioxidants and Radical Scavengers in the ABTS Assay. *Free Radical Res.* **2004**, *38*, 323–331.
- (58) Utkina, N. K. Antioxidant Activity of Aromatic Alkaloids From the Marine Sponges *Aaptos aaptos* and *Hyrtilis SP.* *Chem. Nat. Compd.* **2009**, *45*, 849–853.
- (59) Urmos, J.; Sharma, S. K.; Mackenzie, F. T. Characterization of Some Biogenic Carbonates With Raman-Spectroscopy. *Am. Mineral.* **1991**, *76*, 641–646.
- (60) Takeuchi, H.; Harada, I. Normal Coordinate Analysis of the Indole Ring. *Spectrochim. Acta Part A* **1986**, *42*, 1069–1078.
- (61) Billes, F.; Podea, P. V.; Mohammed-Ziegler, I.; Toşa, M.; Mikosch, H.; Irimie, D.-F. Formyl- and Acetylindols: Vibrational Spectroscopy of an Expectably Pharmacologically Active Compound Family. *Spectrochim. Acta Part A* **2009**, *74*, 1031–1045.
- (62) Vikram, K.; Mishra, S.; Srivastava, S. K.; Singh, R. K. Low Temperature Raman and DFT Study of Creatinine. *J. Mol. Struct.* **2012**, *1012*, 141–150.
- (63) Clark, R. J. H.; Dines, T. J. Resonance Raman Spectroscopy, and Its Application to Inorganic Chemistry. *New Analytical Methods* (27). *Angew. Chem., Int. Ed. Engl.* **1986**, *25*, 131–158.
- (64) Long, D. A., Survey of Light-scattering Phenomena. In *The Raman Effect*; John Wiley & Sons, Ltd.: Bradford, U.K., 2002; pp 3–18.
- (65) Long, D. A., Classical Theory of Rayleigh and Raman Scattering. In *The Raman Effect*; John Wiley & Sons, Ltd.: Bradford, U.K., 2002; pp 31–48.
- (66) Long, D. A., Introduction to Theoretical Treatments of Incoherent Light Scattering. In *The Raman Effect*; John Wiley & Sons, Ltd.: Bradford, U.K., 2002; pp 19–29.
- (67) De Oliveira, L. F. C.; Dantas, S. O.; Vellozo, E. S.; Santos, P. S.; Ribeiro, M. C. C. Resonance Raman Investigation and Semi-empirical Calculation of the Natural Carotenoid Bixin. *J. Mol. Struct.* **1997**, *435*, 101–107.
- (68) Koyama, Y.; Takatsuka, I.; Nakata, M.; Tasumi, M. Raman and Infrared Spectra of the All-trans, 7-cis, 9-cis, 13-cis and 15-cis isomers of  $\beta$ -carotene: Key bands Distinguishing Stretched or Terminal-bent Configurations Form Central-bent Configurations. *J. Raman Spectrosc.* **1988**, *19*, 37–49.
- (69) Kazlauskas, R.; Murphy, P. T.; Quinn, R. J.; Wells, R. J. Aplysinopsin, a New Tryptophan Derivative From a Sponge. *Tetrahedron Lett.* **1977**, *18*, 61–64.

(70) Pauletti, P. M.; Cintra, L. S.; Braguine, C. G.; Filho, A. A. d. S.; Silva, M. L. A. e.; Cunha, W. R.; Januário, A. H. Halogenated Indole Alkaloids from Marine Invertebrates. *Mar. Drugs* **2010**, *8*, 1526–1549.

(71) Putz, A.; König, G. M.; Wagele, H. Defensive Strategies of Cladobranchia (Gastropoda, Opisthobranchia). *Nat. Prod. Rep.* **2010**, *27*, 1386–1402.

(72) Koh, E. G. L.; Sweatman, H. Chemical Warfare Among Scleractinians: Bioactive Natural Products From *Tubastraea Faulkneri* Wells Kill Larvae of Potential Competitors. *J. Exp. Mar. Biol. Ecol.* **2000**, *251*, 141–160.

(73) Bayati, M. R.; Golestani-Fard, F.; Moshfegh, A. Z. Photo-Degradation of Methylene Blue Over V<sub>2</sub>O<sub>5</sub>-TiO<sub>2</sub> Nano-Porous Layers Synthesized by Micro Arc Oxidation. *Catal. Lett.* **2010**, *134*, 162–168.

(74) Conte, V.; Floris, B. Vanadium Catalyzed Oxidation With Hydrogen Peroxide. *Inorg. Chim. Acta* **2010**, *363*, 1935–1946.

(75) Turro, N. J.; Ramamurthy, V.; Scaiano, J. C. *Principals of Molecular Photochemistry: An Introduction*; University Science Books: Sausalito, CA, USA, 2009.